

AD/A-005 275

LASER RANGEFINDER, AN/GVS-5 (XE-2)

Richard J. Newton, et al

Army Electronics Command  
Fort Monmouth, New Jersey

September 1974

DISTRIBUTED BY:

**NTIS**

National Technical Information Service  
U. S. DEPARTMENT OF COMMERCE

UNCLASSIFIED

SECURITY CLASSIFICATION OF THIS PAGE (When Data Entered)

REPORT DOCUMENTATION PAGE		READ INSTRUCTIONS BEFORE COMPLETING FORM
1. REPORT NUMBER ECOM-4256	2. GOVT ACCESSION NO.	3. RECIPIENT'S CATALOG NUMBER
4. TITLE (and Subtitle) LASER RANGEFINDER, AN/GVS-5 (XE-2)	5. TYPE OF REPORT & PERIOD COVERED Final Technical Report	6. PERFORMING ORG. REPORT NUMBER
		6. CONTRACT OR GRANT NUMBER(s)
7. AUTHOR(s) Richard J. Newton, Frederick A. Kobylarz, Richard D. Brady, Richard P. Tuttle	8. PERFORMING ORGANIZATION NAME AND ADDRESS US Army Electronics Command ATTN: AMSEL-CT-L-A Fort Monmouth, New Jersey 07703	10. PROGRAM ELEMENT, PROJECT, TASK AREA & WORK UNIT NUMBERS 186 62704 A 199 02 11
11. CONTROLLING OFFICE NAME AND ADDRESS US Army Electronics Command ATTN: AMSEL-CT-L Fort Monmouth, New Jersey 07703	12. REPORT DATE September 1974	13. NUMBER OF PAGES 34
	14. MONITORING AGENCY NAME & ADDRESS (if different from Controlling Office)	15. SECURITY CLASS. (of this report) Unclassified
16. DISTRIBUTION STATEMENT (of this Report) Distribution approved for public release; distribution unlimited.		15a. DECLASSIFICATION/DOWNGRADING SCHEDULE
17. DISTRIBUTION STATEMENT (of the abstract entered in Block 20, if different from Report)		
18. SUPPLEMENTARY NOTES <p style="text-align: center;">Reproduced by <b>NATIONAL TECHNICAL INFORMATION SERVICE</b> US Department of Commerce Springfield, VA. 22151</p>		
19. KEY WORDS (Continue on reverse side if necessary and identify by block number) Laser rangefinder; AN/GVS-5 (XE-2); Neodymium laser; Krypton flashlamps; Lithium niobate; Silicon avalanche detector; Hybrid counter		
20. ABSTRACT (Continue on reverse side if necessary and identify by block number) This report describes the effort to design, fabricate, and test a hand-held laser rangefinder weighing less than 5 pounds. The effort was initiated in early 1970 when the technology had achieved a potential for success. The use of Nd:YAG in the laser transmitter (which requires less input energy than previous rangefinders using a ruby transmitter) and the development of a highly sensitive, temperature compensated, silicon avalanche receiver permitted a tenfold reduction in weight of the battery, power supply, pulse forming		

DD FORM 1 JAN 73 1473 EDITION OF 1 NOV 65 IS OBSOLETE

Unclassified  
SECURITY CLASSIFICATION OF THIS PAGE (When Data Entered)

Unclassified

SECURITY CLASSIFICATION OF THIS PAGE(When Data Entered)

network and the laser transmitter as compared to previous designs. In addition, a further significant reduction in weight was obtained by the use of Medium Scale Integrated (MSI) electronics in hybrid packages for the majority of circuitry used in the rangefinder. In late 1972 fabrication and testing of three XE-2 model rangefinders was completed. The XE-2 utilizes a 7 x 50 optical system, weighs 4 3/4 pounds, and ranges to 10 km with an error of + 10 m. These models not only demonstrated technical feasibility of a Hand-Held Laser Rangefinder (HHLR), but established a practical, economic, maintainable and reliable design approach for many military and civilian applications.

Unclassified

SECURITY CLASSIFICATION OF THIS PAGE(When Data Entered)

## CONTENTS

Paragraph		<u>Page</u>
1	INTRODUCTION . . . . .	1
2	LASER RANGEFINDER, AN/GVS-5 (XE-2) . . . . .	2
2.1	Configuration . . . . .	2
2.2	Optics . . . . .	3
2.3	Laser Transmitter . . . . .	7
2.4	Receiver . . . . .	11
2.5	Counter . . . . .	23
2.6	Electronics . . . . .	25
2.7	Operation . . . . .	27
3	CONCLUSION . . . . .	28

## FIGURES

		<u>Page</u>
Figure 1.	Characteristics of the Hand-Held Laser Range- finder (XE-2) . . . . .	3
2.	Laser rangefinder in the hand-held mode . . . . .	4
3.	Through the Eyepiece of the Rangefinder . . . . .	5
4.	Optical system - AN/GVS-5 (XE-2) . . . . .	6
5.	Laser Transmitter - Schematic . . . . .	7
6.	Laser Transmitter - Assembly . . . . .	9
7.	Laser Transmitter - Open view . . . . .	10
8.	Laser performance: Xenon vs Krypton flashlamps . . . . .	12
9.	Laser performance: Clear quartz vs UV absorbing envelopes . . . . .	13
10.	Reflectivity of Silver and Gold . . . . .	14
11.	Laser performance: Silver vs Gold cavity . . . . .	15
12.	Laser performance as a function of resonator output reflectivity . . . . .	16
13a.	Detector evaluation summary . . . . .	20
13b.	Range performance . . . . .	21
14.	Typical preamplifier performance characteristics . . . . .	23
15.	Schematic of entire receiver circuitry . . . . .	24
16.	Range counter diagram . . . . .	25
17.	Hybrid range counter . . . . .	26
18.	High voltage power supply . . . . .	27
19.	Low voltage power supply . . . . .	28

## PREFACE

The internal ECOM development of the hand-held laser rangefinder was performed under task number IS6 62704 A 199 02 11 (Very Lightweight Laser Rangefinder program). The objective of the laser rangefinder program is to develop small, lightweight laser ranging/illuminating equipment. Toward this end, the Laser Rangefinder, AN/GVS-5 was developed. The authors wish to acknowledge the following individuals who aided in the development of the laser rangefinder: Dr. H. J. Merrill and Mr. R. Mirarchi for their guidance, moral support, and aid in carrying out the development; Mr. John Strozyk for his aid in support of the laser development; Mr. Norman Yeamans for his support in flashtube technology; Mr. Edward Hughes, machinist, whose ingenuity and perseverance made the fabrication possible; Mr. John Ransom whose response to the innumerable design reviews and changes made possible a final package that worked; Mr. William Matler whose aid in fabrication and testing of the electronics was of significant value; Major A. MacDonald and Major A. Moi of the US Army Infantry School, Fort Benning, GA for their continuous evaluation and critique of the proposed designs.

## NOTICES

### Disclaimers

The findings in this report are not to be construed as an official Department of the Army position, unless so designated by other authorized documents.

The citation of trade names and names of manufacturers in this report is not to be construed as official Government indorsement or approval of commercial products or services referenced herein.

### Disposition

Destroy this report when it is no longer needed. Do not return it to the originator.

ADVISORY	
RTIS	
DSC	
UNCLASSIFIED	
JUSTIFICATION	
BY	
DISTRIBUTION	
Dist.	
A	

ESC-PN 5700-43

V

## 1. INTRODUCTION

1.1 The purpose of this effort was to design and fabricate a small, lightweight hand-held laser rangefinder (HHLR) weighing less than 5 pounds, and to determine overall feasibility and practicality of meeting the requirements for an infantry device. As the required technology was sufficiently in hand in early 1970, an effort was initiated at ECOM for the development of the HHLR.

1.2 The development of the HHLR required careful consideration of those factors affecting the overall weight of the device. Previous rangefinders containing ruby transmitters were heavy primarily because of the large input energy (100 to 300 J) required to obtain a useable laser output. The use of Nd:YAG in the transmitter of the HHLR reduced the required input energy to a nominal 5 J. A penalty was incurred, however, in shifting to the  $1.06\mu$  wavelength laser. Photodetectors are generally less sensitive in this spectral region. This problem was mitigated by the development of a highly sensitive, temperature compensated, silicon avalanche-receiver system. This receiver provided a constant gain and low false alarm rate while compensating for varying noise conditions and laser signal levels due to range and detector sensitivity variations. The use of Nd:YAG in the laser transmitter and the development of the new receiver resulted in a tenfold reduction in weight of the battery, power supply, pulse forming network, and the laser transmitter. In addition, a significant reduction in weight was obtained by the use of Medium Scale Integrated (MSI) electronics in hybrid packages for the majority of circuitry used in the rangefinder.

1.3 These developments were incorporated into the HHLR together with proven design techniques obtained from earlier rangefinder programs. Continuing attention was paid to simplicity of approach within the constraints of system noise, interface parameters, and the required operational characteristics.

1.4 Since this was the first hand-held laser rangefinder, human factors considerations had not been previously defined and therefore were investigated. Three specific configurations were reviewed for possible use, namely: rifle, camera, and binocular. The rifle configuration, while enjoying the greatest user familiarity, was discarded because it required the most

structure, a critical center of gravity (balance), and was difficult to back pack. The camera configuration, while significantly increased over the rifle format (greater packing density and ease in aiming), would have required a more complex, folded, optical system. The binocular configuration was chosen as having the best format for hand-held operation. It allowed for simplicity of internal design and required the least amount of physical structure. Initial tests, conducted in the laboratory, indicated that in the prone position, the majority of the operators could point a 5-pound binocular to within one mil accuracy.

1.5 Another critical area of concern in the design of the rangefinder was the manner in which multiple signal returns would be processed. The design approach selected was a combination of continuously variable minimum range gate (0.2-3.0 km) followed by a first pulse counter. This approach was considered adequate for infantry usage because of the short ranges involved and the small number of signal returns on the average. Multiple target storage was determined to be undesirable because of high energy consumption of high speed counters or shift registers. However, should high speed MOS circuits become available, the target storage solution would be more attractive.

1.6 Using these general approaches and ten years of previous experience in the design of laser devices (AN/GVS-1 series), three models of the AN/GVS-5 (XE-2) rangefinder were designed, fabricated, and tested. The main characteristics of the HHLR are given in Figure 1.

## 2. LASER RANGEFINDER, AN/GVS-5 (XE-2)

### 2.1 Configuration

2.1.1 The dimensional outline of the XE-2 was determined by several factors: the length by the 7 X 50 optical system, the height by the optical system and the power supply, and the width by the optical system with transmitter and receiver. The overall shape was in a binocular format.

2.1.2 The design approach called for the transmitter assembly on the one side of the optics and the receiver assembly on the other to provide the maximum possible noise isolation. With this division of sub-assemblies, components were contoured to allow for the design of an easily hand-held

Maximum Range	10 km
Range Accuracy	$\pm 10$ m
Maximum Ranging Rate	1 per second
Sighting Optics	7 x 50 with mil scale
Weight (including battery)	4 3/4 lbs
Battery	NiCad, rechargeable
Rangings per Battery Charge	400
Range Display	Light Emitting Diode display in sighting optics
Minimum Range Gate	0.2 - 3.0 km

Figure 1. Characteristics of the Hand-Held Laser Rangefinder (XE-2).

package which conformed to a binocular format. The external case was molded from a high impact plastic (KYDEX) with a textured surface for ease of hand-holding (see Figure 2).

## 2.2 Optics

2.2.1 The optical layout was based upon the field proven design of the AN/GVS-1 series of rangefinders. A Galilian collimating telescope was used to reduce the laser beam divergence, and a co-axial system was used for the receiver and sighting functions.

2.2.2 The collimating telescope has a 4 power magnification with a 2.5 cm f/1.25 coated objective. The sighting-receiving optics consists of a standard 7 X 50 optical system with a 1.06 $\mu$  beam splitting cube attached to the erecting prism cluster. Located to the side of the beam splitting cube and in front of the detector is a 2 mrad field stop, a collimating lens, and a 100  $\text{\AA}$  band-pass filter. The field stop is aligned to the sighting reticle and cemented in place on the prism cluster. The range display is placed at the lower portion of the reticle. The display consists of four 7-segment red light emitting diodes (LED) (see Figure 3). A schematic representation of the optical system is shown in Figure 4. The housing for the optical system is a magnesium casting.



Figure 2. Laser Rangefinder in the hand-held mode.



Figure 3. Through the Eyepiece of the Rangefinder.

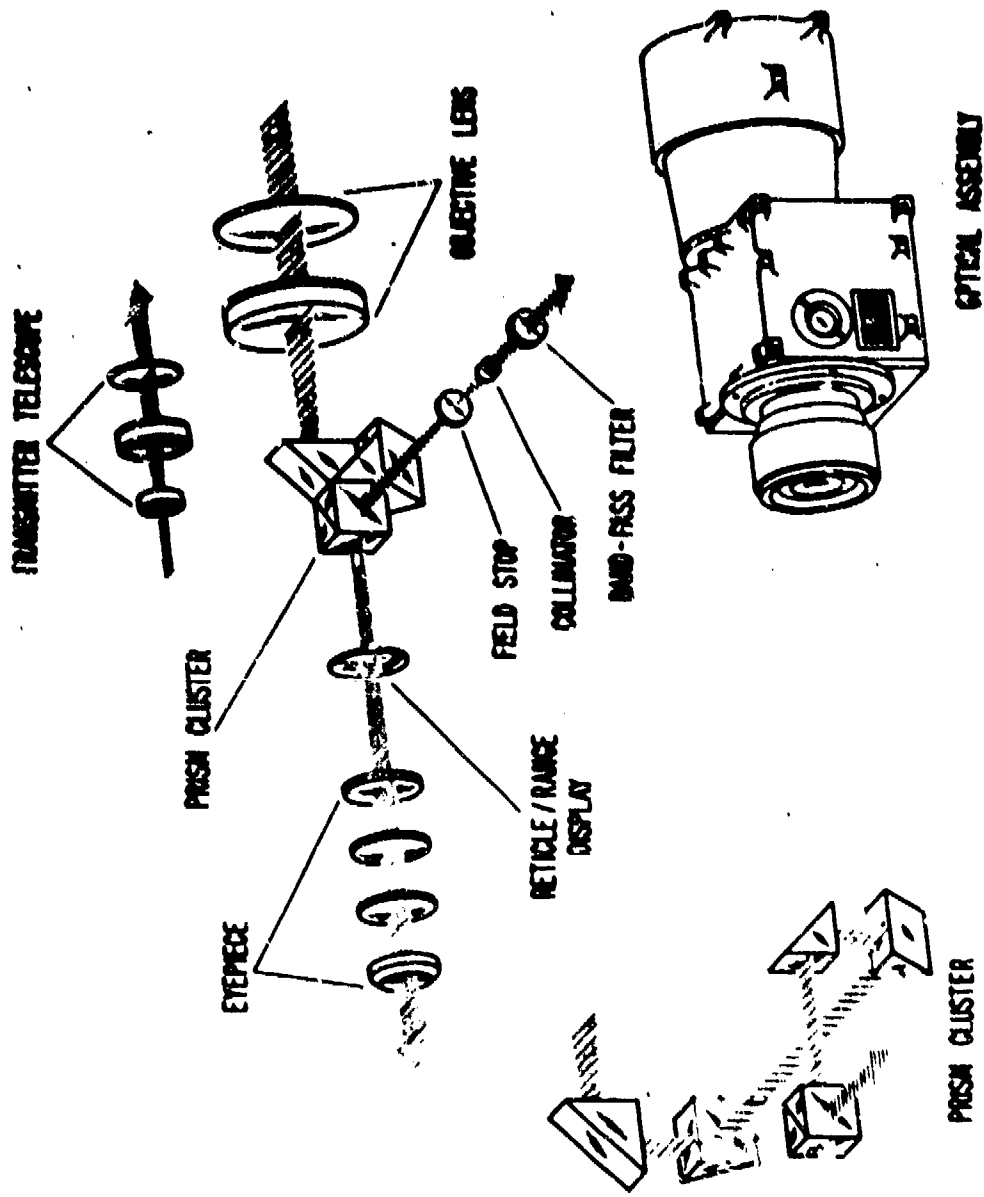


Figure 4. Optical system - AN/GVS-5 (XE-2).

2.2.3 Transmitter and receiver-sighting optics are boresighted by moving the negative element of the collimating telescope. The optical transmission of the receiver system is 50% and the total optical system weighs 2 pounds

### 2.3 Laser Transmitter

#### 2.3.1 Introduction.

The miniaturized laser transmitter design evolved through trade-offs of size, cost, and performance. A 5 mm x 30 mm neodymium-doped Yttrium Aluminum Garnet (Nd:YAG) laser rod, as the dominating component of the laser transmitter, presented the most favorable of these trade-offs. Although a 5 mm x 30 mm laser rod was utilized, further work should be performed with less expensive 3 mm x 30 mm laser rods to upgrade performance.

#### 2.3.2 Construction.

The laser transmitter is a small in-line laser device 6.4 cm in length. A schematic of the laser transmitter is shown in Figure 5.

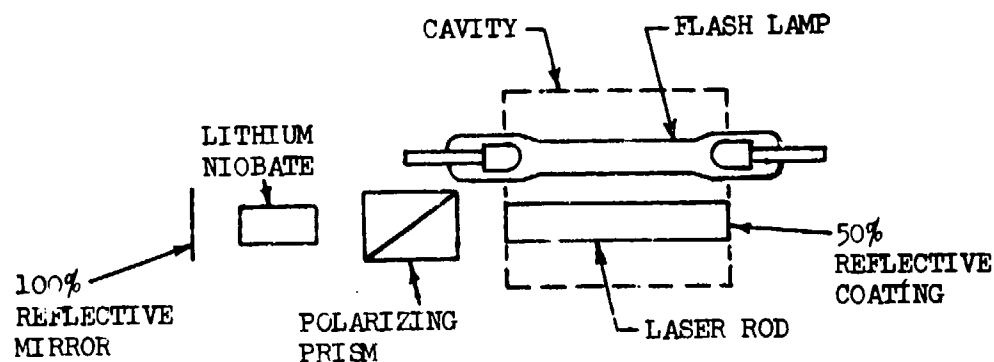


Figure 5. Laser Transmitter - Schematic.

The resonator consists of a 100% reflective flat mirror at the rear of the laser transmitter and a 50% reflective coating on the front surface of the laser rod. The alignment of the two reflective surfaces is critical and must be maintained within a few seconds of arc. The Nd:YAG laser rod used is 5 mm x 30 mm. The rod is pumped in a close coupled, silver coated quartz intersecting circle cavity by a high pressure (1200 torr) Krypton lamp 30 mm in arc length and 3 mm in bore with a clear fused quartz envelope. This lamp was selected because its emission spectrum more closely matches the excitation spectrum of Nd:YAG than the normally used Xenon lamp. A Pockel Cell Q-switch was used which consisted of an air spaced Glan-Thompson calcite polarizing prism and a Lithium Niobate crystal. The laser transmitter assembly is shown in Figures 6 and 7.

### 2.3.3 Operation.

2.3.3.1 Energy is provided to the lamp by a small pulse forming network (PFN). The three ounce capacitor used in the PFN was a specially developed metalized Mylar unit for lasers having a very high energy storage-to-weight ratio at low voltages. This was achieved by new technology in film dielectrics and the development of a self healing Mylar film. The capacitor is capable of an energy density of greater than 40 J/lb at 1000 V. The power supply for charging the PFN uses a highly efficient scheme for charging a capacitor. The efficiency of this supply is about 80%.

2.3.3.2 The Lithium Niobate crystal rotates the plane of polarization of transmitted light as a function of applied voltage. Based upon the polarization of the laser energy, the polarizing prism either keeps the energy in the transmitter (high-Q) or releases the energy from it (low-Q). During the pumping of the laser rod, a high loss/low-Q condition is maintained. The flashlamp output is delayed about 40 microseconds after the trigger pulse. The pumping is completed after a total of about 80 microseconds. An additional 30  $\mu$ s are allowed for flashlamp quenching noise to decay, then the Q-switch is rapidly (10 ns) brought to the low loss/high-Q condition, and the laser pulse is generated. The Q-switching process is done automatically by the sequencing electronics. When the PFN is charged to the proper level, a signal is sent to the sequencing electronics. The sequencing electronics generates a 110  $\mu$ s pulse. The leading edge of the pulse triggers

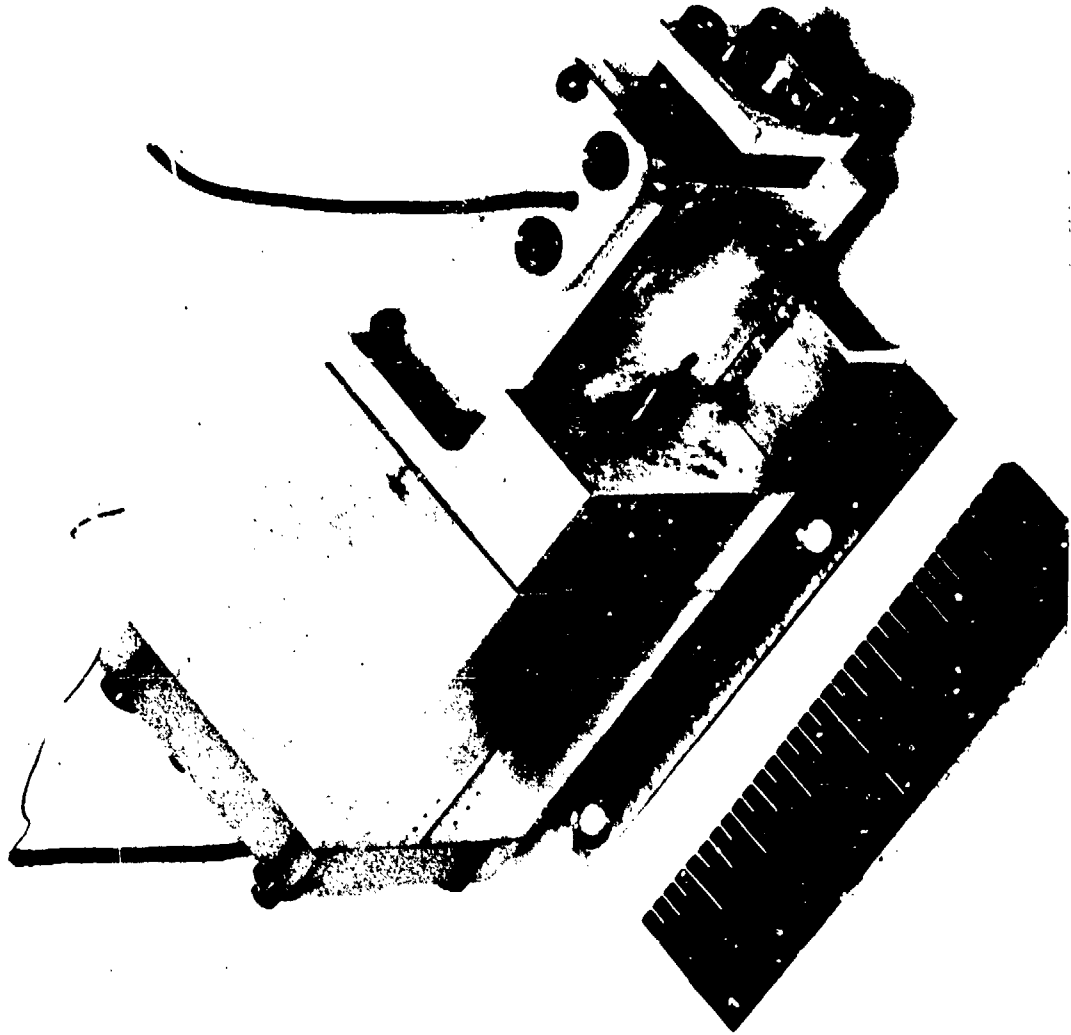


Figure 6. Laser Transmitter - Assembly.



Figure 7. Laser Transmitter - Open view.

the flashlamp. The trailing edge triggers a Krypton, a fast cold cathode tube, which removes the bias voltage from the Q-switch and allows laser action.

#### 2.3.4 Optimization

2.3.4.1 In the interest of conserving the rangefinder battery power, it was decided to optimize the laser output at a 5 J input.

2.3.4.2 The first area of optimization was the flashlamp. Above the 4 J level, a high pressure Krypton-filled lamp operates more efficiently in the system than does a high pressure Xenon-filled lamp (see Figure 8). With the high pressure Krypton, a clear fused quartz envelope yields more output energy than does a UV absorbing envelope (see Figure 9).

2.3.4.3 From Figure 10, silver is shown to be more reflective than gold, particularly in the pump bands of Nd:YAG (Reflectivity data from Handbook of Chemistry and Physics, Robert C. Weast, Editor, Chemical Rubber Co., Ohio, 1967). Silver should, therefore, be a better pump cavity reflector than gold. Figure 11 shows that a silver coated pump cavity is more efficient than a gold coated cavity.

2.3.4.4 The final area of optimization considered is the reflectivity at the output end of the laser resonator that will yield maximum laser output at a 5 J input. Figure 12 shows that in the normal mode operation a 75% output reflectivity provides maximum output energy. However, when the laser transmitter is operated in the Q-switched mode, a 50% output reflectivity provides the maximum output. The final optimized laser transmitter had an output of 15 mJ with a nominal 5 J input. The pulse width was about 7 ns yielding approximately 2 MW peak power.

#### 2.4 Receiver

2.4.1 For given transmitter characteristics (output energy and pulse width), the receiver defines the overall rangefinder capabilities. Thus, to obtain the desired objectives (sensitivity, small size on power requirements, and maximum capability), an intensive analysis was performed to select the optimum detector; design, optimize, and fabricate a low noise preamplifier; design a time programmed gain circuit to avoid false signals (detection) due to atmospheric backscatter; and to provide a normalized stop signal output to the counter.

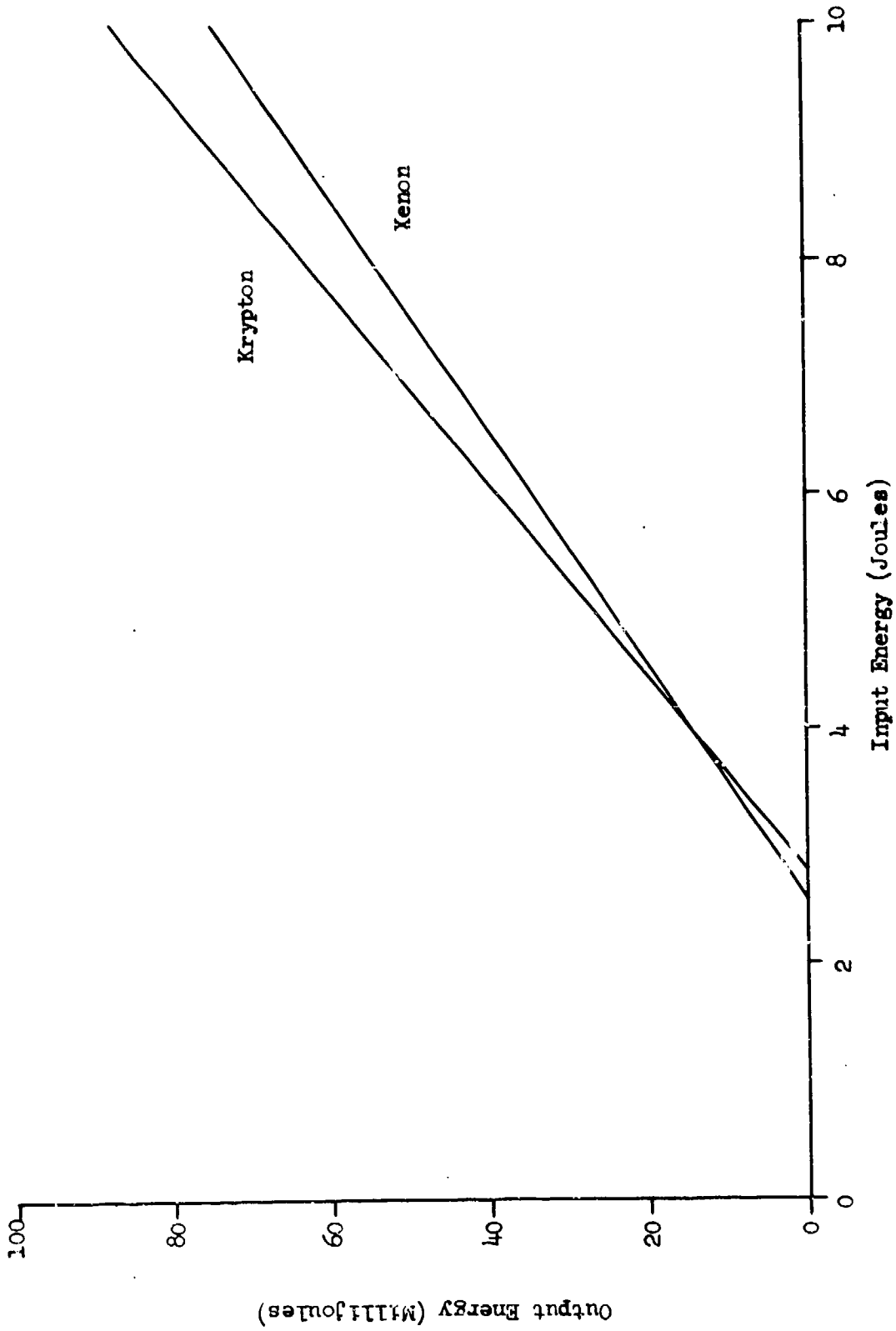


Figure 8. Laser performance: Xenon vs Krypton flashlamps.

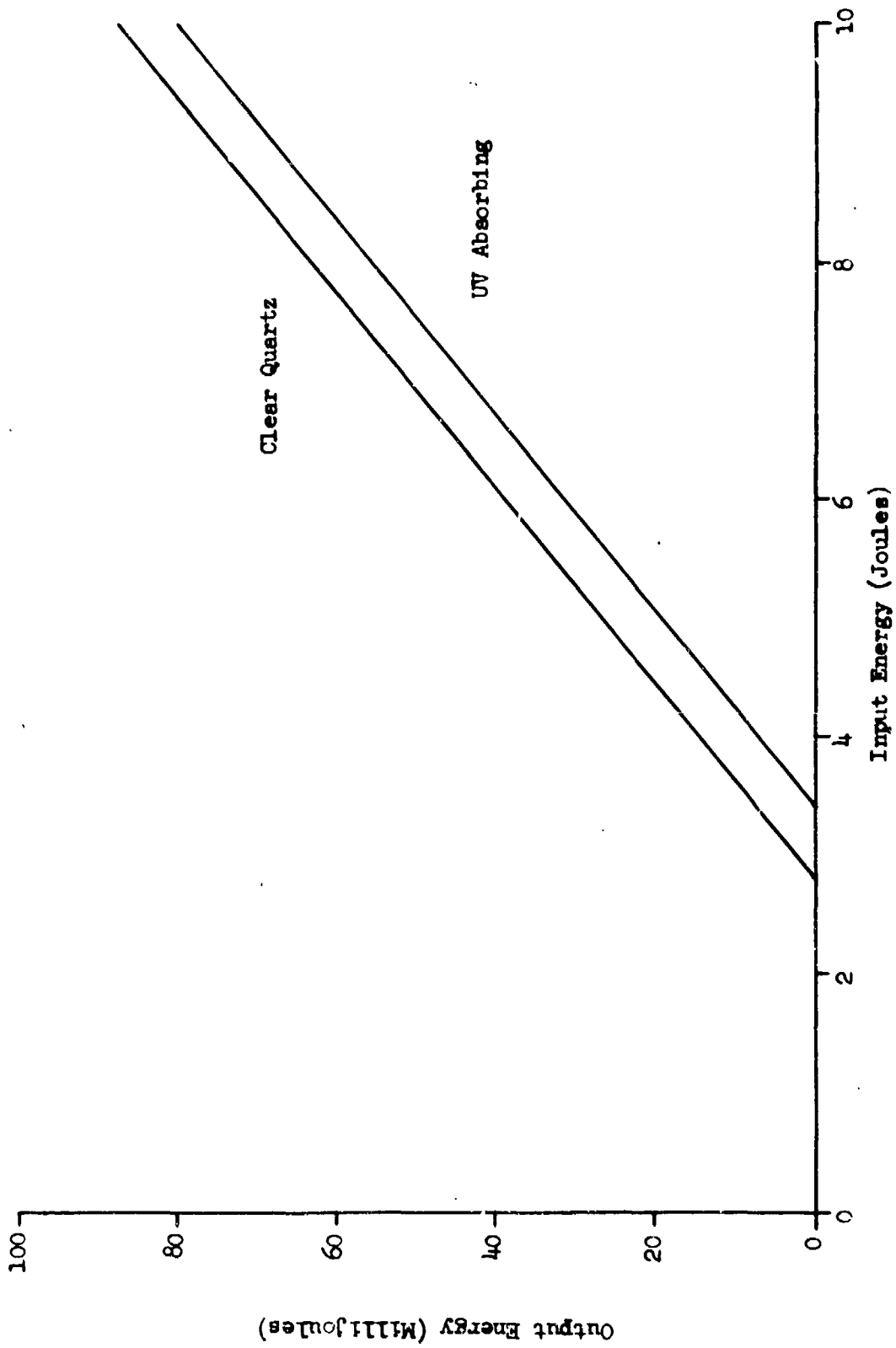


Figure 9. Laser performance: Clear Quartz vs UV absorbing envelopes.

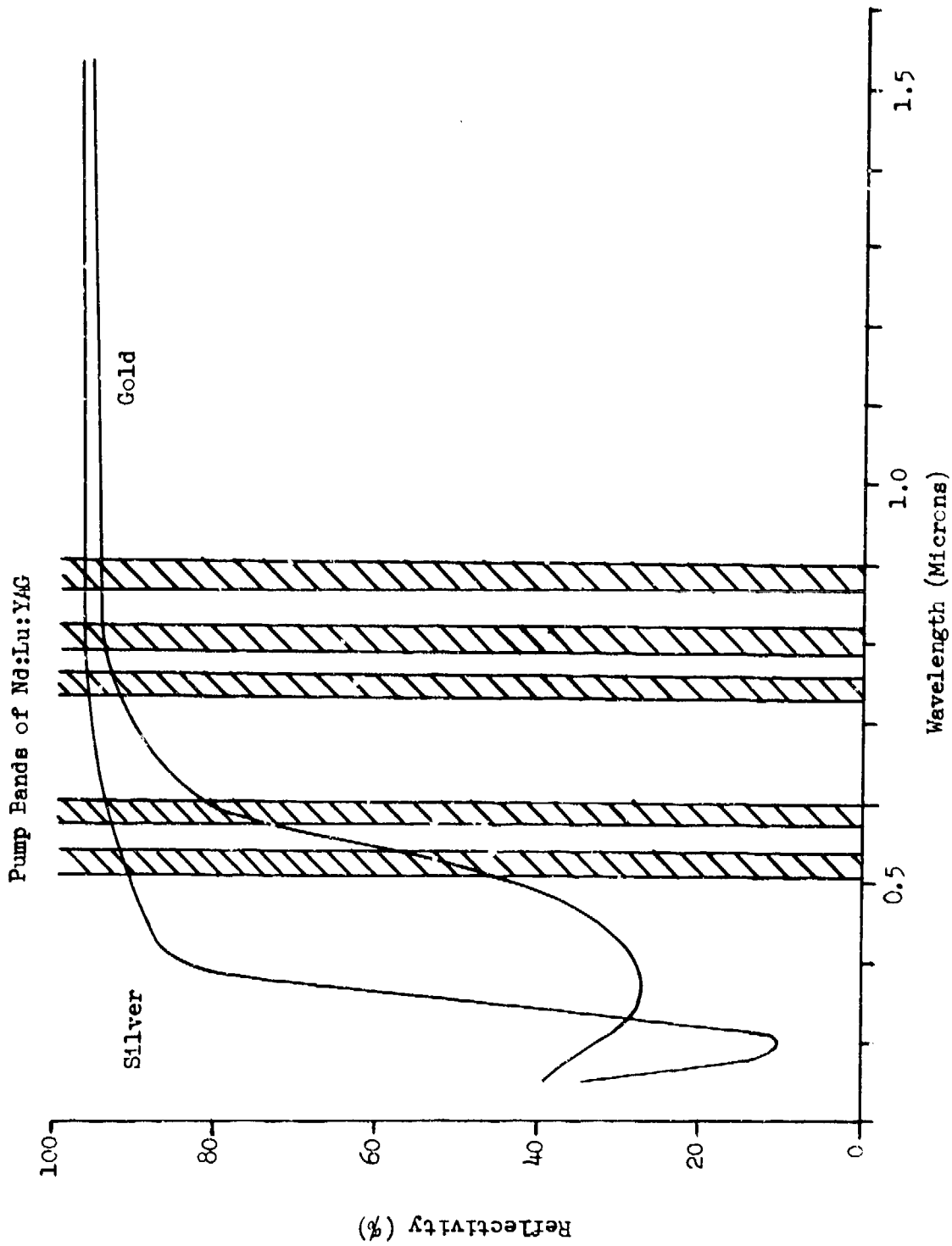


Figure 10. Reflectivity of Silver and Gold.

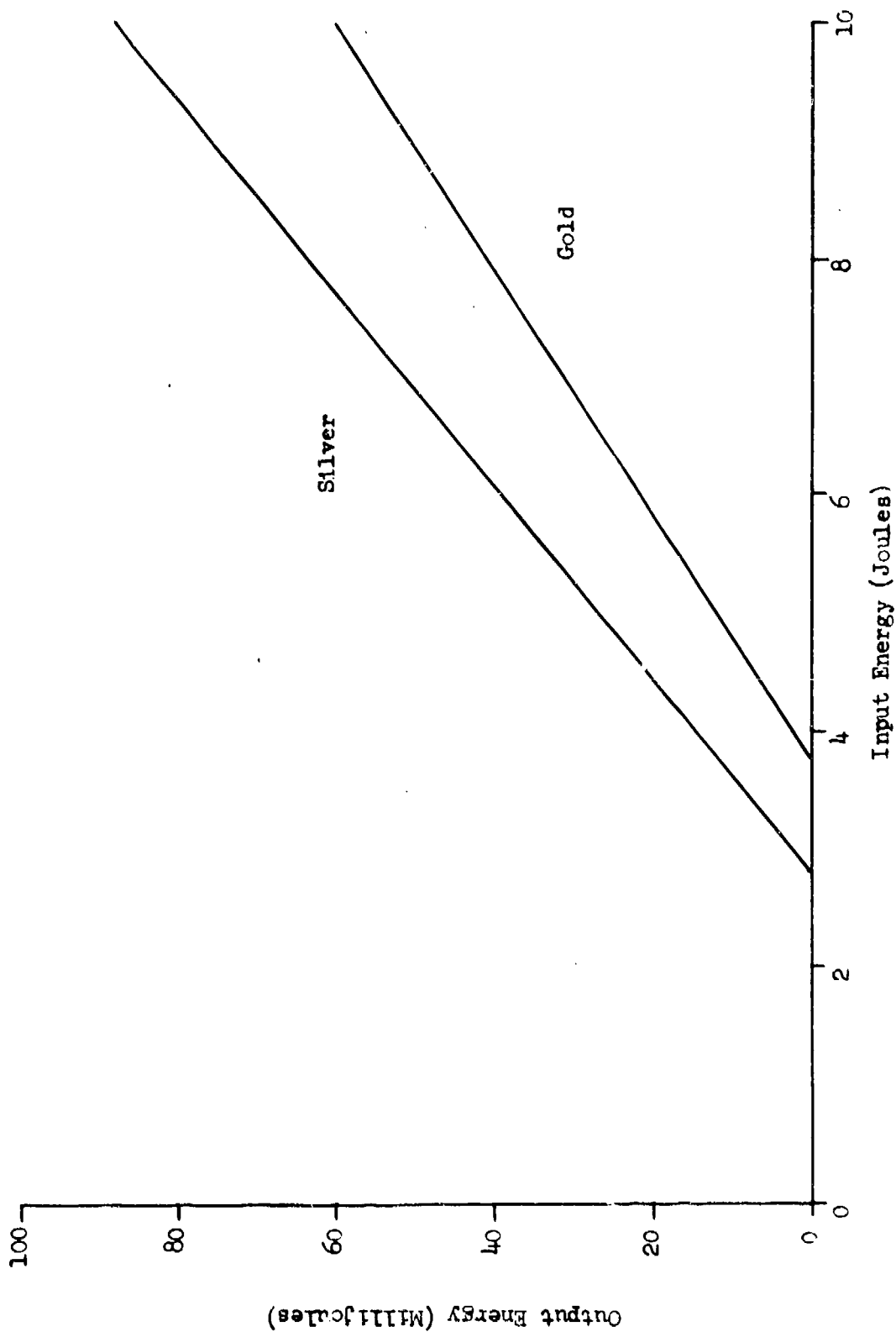


Figure 11. Laser performance: Silver vs Gold cavity.

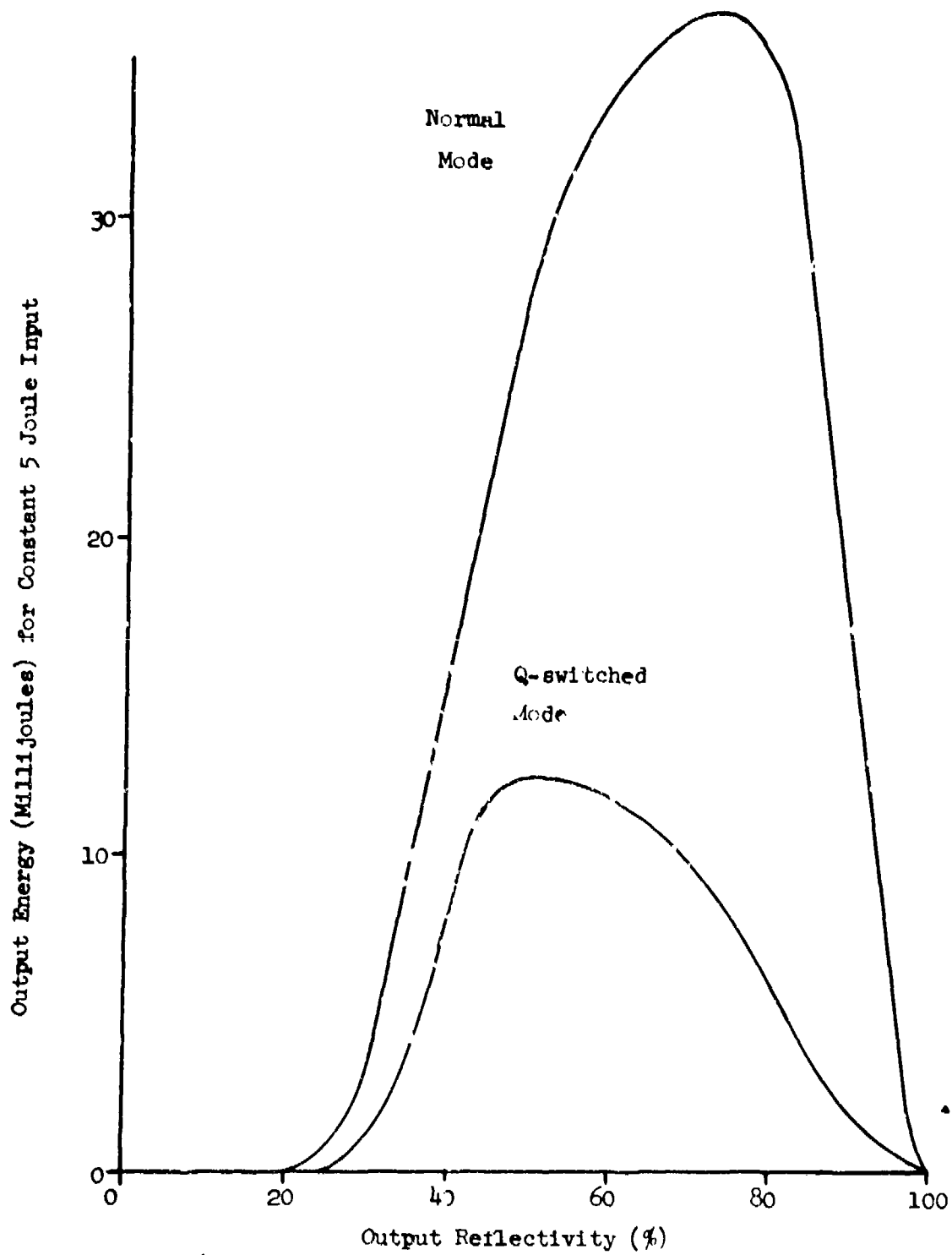


Figure 12. Laser performance as a function of resonator output reflectivity.

The signal power level at the detector is given by the following:

$$P_s = \frac{P_t A_r' \rho}{\pi R^2} \exp \{-2\sigma R\} \quad (1)$$

where

$P_s$  = signal power in watts,

$P_t$  = transmitted power in watts =  $2 \times 10^6$  W,

$\rho$  = target reflectivity = 0.1,

$\sigma$  = atmospheric extinction coefficient = 0.9 km @ 1.06 $\mu$ ,

$R$  = range in km,

$A_r'$  = effective receiver area = 6 cm<sup>2</sup> (includes losses due to optics and bandpass filter).

To determine the maximum range capability, the receiver operating parameters (detector, preamp and statistical data) must be evaluated.

#### 2.4.2 Detector evaluation.

2.4.2.1 Detectors that exhibit useable sensitivity at 1.06  $\mu$  are photoemissive devices (S-1 photomultiplier tube) and solid state devices (photodiodes and avalanche detectors). The avalanche detector differs from the photodiode in that photo induced current can be multiplied internally when biased close to breakdown (avalanche). At avalanche, dark current increases rapidly with an increase in the number of noise counts with large amplitudes.

2.4.2.2 To evaluate the detectors' performance (for maximum signal-to-noise ratio), all possible noise sources must be included. These noise sources limit the minimum detectable signal of the receiver. There are three dominant noise sources within the optical receiver: noise determined by background radiation; noise generated by the detector preamplifier; and noise generated due to dark current.

2.4.2.3 The amount of background power incident on the detector is given by:

$$P_B = H_{\lambda s} \alpha_r^2 A_r' \Delta\lambda \{ \rho/4 + 1/8 \} \quad (2)$$

where

$$H_{\lambda_s} = \text{solar spectral irradiance} = 6 \times 10^{-6} \text{ W/cm}^2\text{-}\lambda \text{ @ } 1.06 \mu,$$

$$\alpha_T = \text{receiver field-of-view} = 2 \text{ mrad},$$

$$\Delta\lambda = \text{optical bandwidth of interference filter} = 100 \text{ \AA}.$$

The noise current induced by the background is given by:

$$i_{n_1}^{-2} = 2eS P_B M_1^Y \Delta f, \quad (3)$$

where

S = sensitivity of detector at unity gain,

$M_1$  = D.C. multiplication at 1.06  $\mu$ ,

$\gamma$  = 2.4 for silicon.

2.4.2.4 The thermal noise due to the preamplifier is given by:

$$i_{n_2}^{-2} = \frac{4k T F \Delta f}{R_f} \quad (4)$$

where

k = Boltzman's constant,

F = noise factor,

$\Delta f$  = electrical bandwidth,

$R_f$  = preamplifier feedback resistance.

The preamplifier equivalent input noise current was measured to be  $2.6 \times 10^{-12} \text{ A}/\sqrt{\text{Hz}}$ .

2.4.2.5 The third source of noise is due to the dark current (bulk and surface). The shot noise due to this leakage current for the silicon avalanche detector is:

$$i_{n_3}^{-2} = 2e [i_1 + i_d M_1^Y] \Delta f \quad (5)$$

where

$i_1$  = surface leakage current,

$i_d$  = bulk leakage current.

2.4.2.6 The apparent change in multiplication is the effect of the greater absorption length of  $1.06 \mu$  radiation. The absorption of photons should occur in the depletion layer of the reversed biased diode; but due to the absorption path length of  $1.06 \mu$  radiation, absorption occurs in the low electric field region.

2.4.2.7 The signal output current of the detector is  $I_s = SP_s M_{lac}$  and the signal-to-noise ratio is expressed as;

$$S/N = \sqrt{\frac{SP_s M_{lac}}{\left[ \frac{4 k T F}{R_f} + 2e \{ I_1 + I_d M_1^Y + S P_B M_1^Y \} \right] \Delta \tau}} \quad (6)$$

An expression for  $M_{opt}$  can be determined from Equation (6).

$$M_{opt} = \frac{4 k T F / R_f + 2 e I_1}{(\gamma - 2) e \{ 2 I_d^- + S P_B^- \}} \quad (7)$$

2.4.2.8 The optimum receiver bandwidth (when detector is operated at optimum gain) was calculated to be 46 MHz. Since the preamplifier can be considered to be a "noisy" filter (when the detector is operated below  $M_{opt}$ ), the optimum bandwidth for this case was calculated to be 23 MHz. As the bandwidth is decreased, the peak signal decreases affecting the statistics involved for probability of detection. For a 23 MHz bandwidth, the required signal-to-noise ratio for  $P_d = 90\%$  is approximately 13/1.

2.4.2.9 The optimum gain (Silicon Avalanche Detector) dependent upon detector quantum efficiency was calculated to be;

$$160 \leq M_{opt} \leq 210.$$

The actual gain was selected such that the overall detector sensitivity was 15 A/W (less than manufacturer's minimum responsivity specification), to meet desired operational characteristics.

2.4.2.10 The results of all detectors evaluated are listed in Figure 13a. The minimum detectable signal (MDS) is given for a 50% probability of detection ( $P_d$ ). As seen in Figure 13a, the optimum device is the silicon avalanche detector. It represents an order of magnitude of improvement at  $M_{opt}$  (minimum) over the germanium avalanche detector and S-1 photomultiplier tube (PMT).

Detector Type	Calculated MDS ( $\times 10^{-9}$ watts)
S-1 PNT	260
Silicon Photodiode	350
Germanium Avalanche	85
Silicon Avalanche	12 @ (15 amps/watt) 7 ( $M_{out}$ )

Figure 13a. Detector evaluation summary.

2.4.2.11 For  $P_d = 90\%$ , the signal-to-threshold ratio is approximately 1.3/1, yielding  $P_s = 16 \mu W$  for the silicon avalanche detector (15 A/W). Substituting back into Equation (1) yields

$$R^2 \exp(1.8 R) = 0.382 \times 10^{-4} / P_s = 2.3 \times 10^3.$$

The maximum range capability for these conditions is  $R_{max} = 3$  km, when the visual range is 3 km. The range capability as a function of visual range is shown in Figure 13b.

### 2.4.3 Electronics

2.4.3.1 The primary design characteristics of the preamplifier were its noise properties, bandwidth and gain. Since the detector behaves as a current source, inserting a load resistor followed by a voltage amplifier will not achieve optimized characteristics. The preamplifier that is designed and used in the XE-2 was of the operational type. The first stage provides stabilized current gain, while the second stage is a stabilized transimpedance amplifier. The preamplifier bandwidth (for large open loop voltage gain) is approximately

$$f_2 = 1/2 \pi R_f C_{cb}$$

where

$C_{cb}$  = collector-base capacitance.

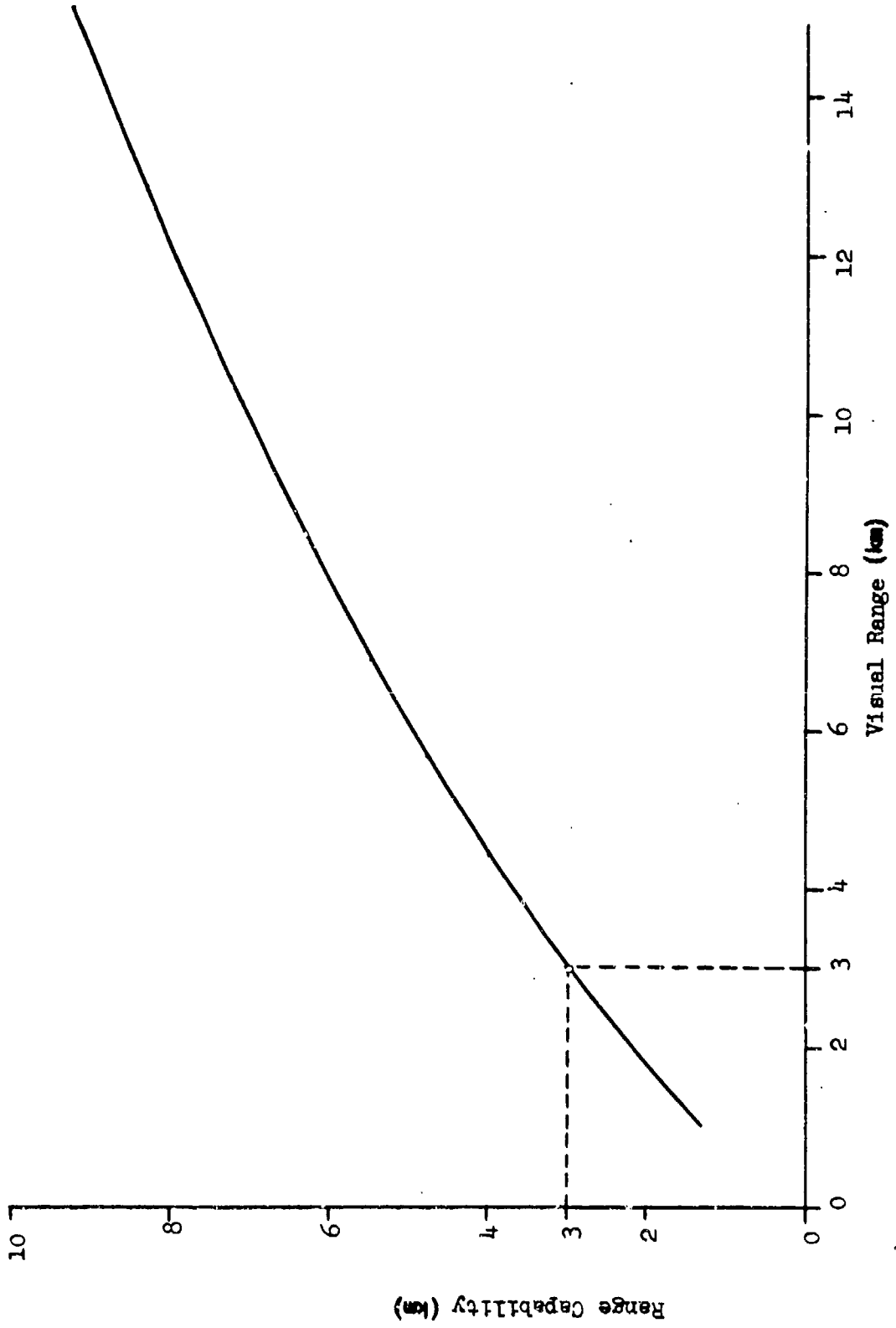


Figure 13b. Range performance.

The preamplifier noise sources (uncorrelated) can be reduced to equivalent noise resistances for current and voltage. These are described as follows:

$$R_{nv} = r_b + r_e/2$$

$$R_{ni} = 2\beta_o r_e$$

where

$r_b$  = base resistance,

$r_e$  = emitter resistance,

$\beta_o$  = current gain =  $n_{fe}$ .

The noise factor of the preamplifier can be approximated by

$$F = 1 + R_{nv}/R_{f1} + \frac{(R_{f2} + r_b + r_e)^2}{R_{ni} R_{f1}}$$

The input transistor was operated at a collector of 300  $\mu$ A; at this level a noise factor of 1.4 was achieved. The typical operating characteristics are given in Figure 14.

2.4.3.2 Input current levels as high as 4 A did not degrade preamplifier performance. The preamplifier signal output is fed into an integrated circuit video amplifier (MC1590G). A method of automatic gain control (AGC) is provided by the manufacturer. Time programmed gain (to prevent atmospheric backscatter detection) is accomplished utilizing a ramp generator and the AGC input. Characteristic of the AGC input is the voltage ( $V_{AGC}$ ) required and the series resistance ( $R_{AGC}$ ), to obtain the desired gain as a function of time. By varying  $V_{AGC}$  (ramp function) for  $R_{AGC} = 33k\Omega$ , the video amplifier gain changes such that the video amplifier signal output remains nearly constant. The gain change was measured and found to fit the equation

$$G(t) = \exp(-2\sigma R)/R^2$$

for ranges to 1.5 km. At 1.5 km the gain is maximum and remains there for an additional 56  $\mu$ s. The AGC input was a negative going ramp since minimum gain occurs at  $V_{AGC} = 1.2$  volts and maximum gain at  $V_{AGC} = 0$  volts. The dynamic range was measured to be greater than 65 dB, with a voltage gain of 150.

Transimpedance	66 k $\Omega$
Bandwidth	23 MHz
Noise Current Spectral Density	2.6 pA/ $\sqrt{\text{Hz}}$

Figure 14. Typical preamplifier performance characteristics.

2.4.3.3 The video amplifier signal output is then fed into a threshold circuit (a 8H80A gate utilized as a monostable). When the peak signal exceeds threshold, a pulse (2.8 V, 70 ns) is used to stop the counter.

2.4.3.4 The detector avalanche voltage varies as a function of temperature with a positive temperature coefficient (increases as temperature increases). In addition, as temperature (T) increases, the leakage current increases (doubles for every 10°C change in temperature). For a constant signal output (sensitivity) and temperature independence, the detector bias voltage must be changed accordingly.

2.4.3.5 The detector temperature compensation scheme employed was the open loop type. Stabilization was achieved with the use of temperature sensitive components whose characteristics change proportionally to the surrounding temperature. The temperature compensation (T-C) network that was evolved consisted of a  $\mu\text{A}723$  voltage regulator, diodes and resistors. The output of the voltage regulator is fed into the dc-dc converter input, and the dc-dc converter output biases the detector to the desired sensitivity. The output signal remained constant to within  $\pm 8\%$  throughout the Military Specifications temperature range.

2.4.3.6 Figure 15 is a schematic of the entire receiver circuitry.

## 2.5 Counter.

2.5.1 The range counter in the XE-2 rangefinder consists of an oscillator, a ripple counter, decoding logic, start-stop logic, and a minimum range gate, fabricated with MSI circuits as shown in the block diagram in Figure 16. The actual hybrid counter is shown in Figure 17. The crystal frequency (14.98554 MHz) was selected so that the decade counters register each cycle as a 10 m range increment. These pulses are gated on and



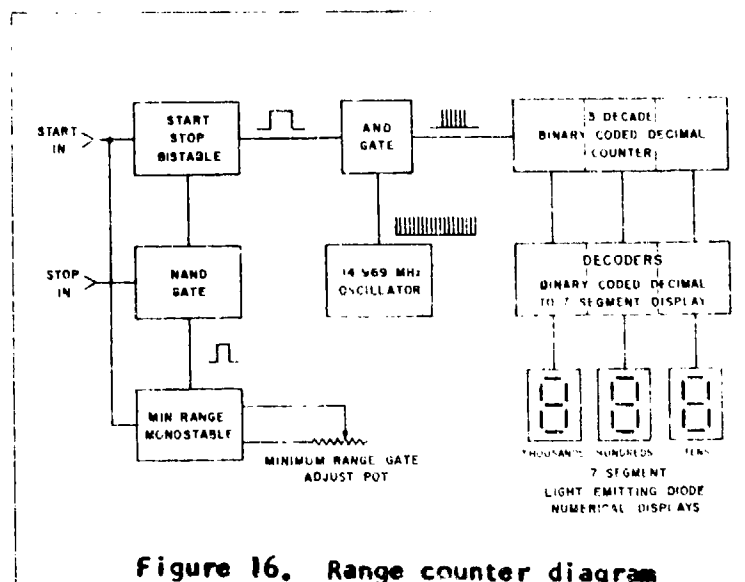


Figure 16. Range counter diagram

off by the start-stop bistable. The stop input to the bistable is additionally gated by the minimum range monostable, allowing the range counter to inhibit receiver stop pulses before the minimum range setting. The Binary Coded Decimal (BCD) counters and the BCD to 7 Segment Decoders are Medium Scale Integrated (MSI) TTL circuits, which contain the equivalent of nearly 500 discrete transistors. These circuits count, store, decode, and drive the display which consists of a miniature 4-digit 7-segment array of light emitting diodes. The entire hybrid counter weighs 0.2 oz, occupies 1.5 square inches, and consumes 1.5 W of power.

2.5.2 The hybrid counter provides many benefits over a discrete component counter; such as, reduced cost, improved reliability, small size, and ease of replacement. The hermetically sealed package contains all of the components associated with the counter except the crystal and display. This allows the unit to be tested on a go-no-go basis and is low enough in cost to be considered a throw-away item.

## 2.6 Electronics.

2.6.1 The power supply in the XE-2 rangefinder uses a constant current, reactive current limiting step-up oscillator design (see Figure 18). Q1 is turned on and charges T1. At a preset level, T1 becomes saturated and Q1 is turned-off. As this occurs, T1 reverses its polarity; current now flows



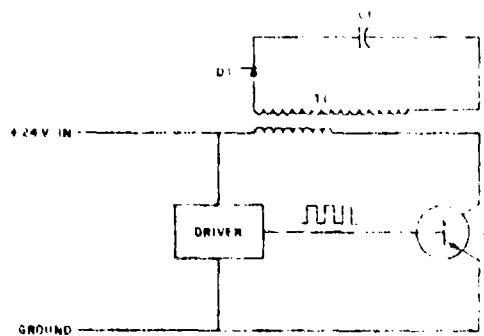


Figure 18. High voltage power supply.

through D1 and contributes charge to the PFN capacitor C1. This cycle is repeated at a 10 kHz rate until C1 has charged to the correct voltage. The Pockel Cell voltage is obtained by sampling the output of T1 and quadrupling it to the desired level. An efficiency of approximately 80% was realized in the power supply.

2.6.2 To improve the efficiency of the low voltage power supplies (12 and 5 V), switching regulators were used instead of resistive regulators. A switching regulator offers the advantages of high efficiency dc-dc voltage conversion, small size and weight, and excellent regulation. Instead of a fixed resistive loss, the pass transistor is either on or off. In operation, when Q1 (see Figure 19) is turned on, current flows through L1 to charge C1. When the output voltage reaches  $V_{ref}$ , Q1 is turned off by the comparator circuit. Current is then fed to the load from the energy stored in both the inductor and the capacitor. When this expenditure of energy drops  $V_C$  below the reference level, Q1 is again turned on and this cycle is repeated. This type of circuit is especially recommended for low voltage circuits (less than 10 V) where regulation losses or rectifier losses become significant.

## 2.7 Operation.

In operation, the operator holds the rangefinder like a pair of binoculars (see Figure 2), centers the reticle on the target, and depresses the fire button. One second later, the laser fires and the range is displayed.

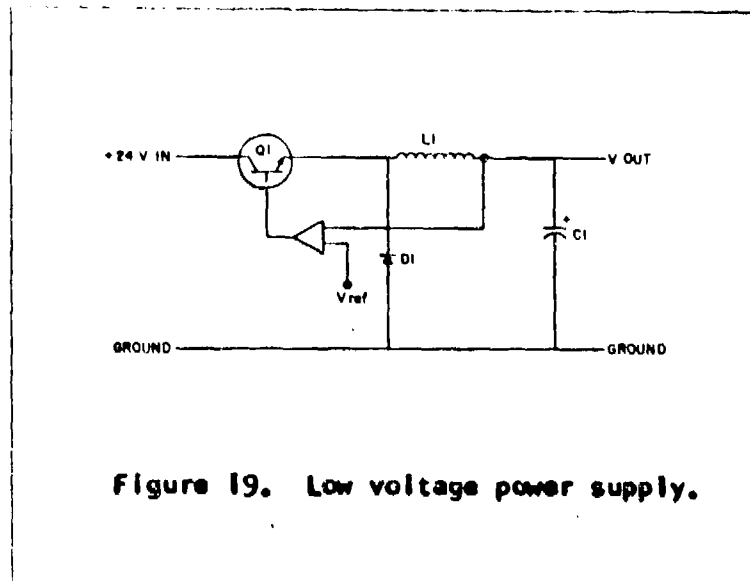


Figure 19. Low voltage power supply.

Figure 3 is a view looking through the eye-piece. The reticle pattern is shown with a one mil circle at the center delineating the laser impact area. The 4-digit LED range display is shown below the reticle.

### 3. CONCLUSION

3.1 Technical feasibility of a hand-held laser rangefinder was demonstrated with the fabrication and testing of the XE-2 model rangefinders. These models established a practical, economical, maintainable and reliable base design approach for many military and civilian applications. Having established these parameters, the AN/GVS-5 Hand-Held Laser Rangefinder is ready for engineering development.